Stabilization Analysis of Neoclassical Tearing Mode in Fusion Plasmas*)

Daiki KURITA, Kozo YAMAZAKI, Hideki ARIMOTO, Tetsutarou OISHI and Tatsuo SHOJI

Nagoya University, Furo-cho, Chikusa-ku, Nagoya 464-8603, Japan

(Received 9 December 2011 / Accepted 11 September 2012)

For the stabilization of neoclassical tearing mode (NTM), Electron Cyclotron Current Drive (ECCD) is used. The change of the EC control efficiency depends on EC modulation width and EC injection phase lag from the O-point of magnetic island. In this work, NTM stabilization by ECCD is analyzed using 1.5-dimensional transport code TOTAL, in which the time variation of magnetic island is described by the modified Rutherford equation. NTM in ITER can be stabilized when the EC phase lag is smaller than 10% and the EC modulation width is around 20%, when the time-averaged EC current and power is fixed.

Keywords: MHD stability control, neoclassical tearing mode, magnetic island, tokamak, ITER

DOI: 10.1585/pfr.7.2403149

1. Introduction

For the achievement of high beta value in tokamak fusion reactors, it is important to control magnetic islands produced by neoclassical tearing mode (NTM) and to suppress resultant plasma confinement degradation [1].

Plasma parameter changes due to NTM are analyzed using time-dependent 1.5-dimensional (1.5-D) transport code TOTAL. In the simulation code, 1-D transport and 2-D equilibrium are analyzed. The time variation of magnetic island is described by the modified Rutherford equation [2].

For the stabilization of NTM, Electron Cyclotron Current Drive (ECCD) is used. The stabilization efficiency of the EC current localization is changed by EC injection phase, position and modulation.

2. Numerical Model

The time evolution of fusion plasma has been calculated using 1.5-dimensional transport code TOTAL. The plasma equilibrium is solved by Apollo code [3], and the anomalous transport coefficient is obtained using the GLF23 transport model package [4]. This package source program can be downloaded from the web site http://w3.pppl.gov/ntcc/GLF/.

2.1 Modified Rutherford equation

The time evolution of NTM island width, W, on the coordinate of the normalized minor radius, ρ, is calculated according to the modified Rutherford equation,

$$\frac{\mathrm{d}w}{\mathrm{d}t} = \Gamma_{\Delta'} + \Gamma_{\mathrm{BS}} + \Gamma_{\mathrm{GGJ}} + \Gamma_{\mathrm{pol}} + \Gamma_{\mathrm{EC}}, \tag{1}$$

$$\Gamma_{\Delta'} = k_{\mathrm{c}} \frac{\eta}{\mu_0} \langle |\nabla\rho|^2 \rangle \frac{1}{\varphi} \frac{\mathrm{d}\varphi}{\mathrm{d}\rho}\bigg|_{ps-w/2}^{ps+w/2}, \tag{2}$$

$$\Gamma_{\mathrm{BS}} = k_{\mathrm{BS}} \eta L_{\mathrm{q}} j_{\mathrm{BS}} \left\langle \frac{|\nabla\rho|}{B_{\mathrm{p}}} \right\rangle \frac{W}{W^2 + W_{\mathrm{d}}^2}, \tag{3}$$

$$\Gamma_{\mathrm{GGJ}} = -k_{\mathrm{GGJ}} \frac{\eta}{\mu_0} \varepsilon_{\mathrm{s}}^2 \beta_{\mathrm{ps}} \frac{L_{\mathrm{q}}^2}{\rho_{\mathrm{s}} L_{\mathrm{p}}} \left(1 - \frac{1}{q_{\mathrm{s}}^2}\right) \langle |\nabla\rho|^2 \rangle \frac{W}{W^2 + W_{\mathrm{d}}^2}, \tag{4}$$

$$\Gamma_{\mathrm{pol}} = -k_{\mathrm{pol}} \frac{\eta}{\mu_0} g(\varepsilon_{\mathrm{s}}, \upsilon_{\mathrm{i}}) \beta_{\mathrm{ps}} \left(\frac{\rho_{\mathrm{pi}} L_{\mathrm{q}}}{L_{\mathrm{p}}}\right)^2 \langle |\nabla\rho|^2 \rangle \frac{W}{W^4 + W_{\mathrm{pol}}^4}, \tag{5}$$

$$\Gamma_{\mathrm{EC}} = -k_{\mathrm{EC}} \eta \frac{L_{\mathrm{q}}}{\rho_{\mathrm{s}}} \left\langle \frac{|\nabla\rho|}{B_{\mathrm{p}}} \right\rangle \eta_{\mathrm{EC}} \frac{I_{\mathrm{EC}}}{a^2} \frac{1}{w^2}, \tag{6}$$

where $\Gamma_{\Delta'}$ is the classical stability index defined as the logarithmic jump of the radial magnetic perturbation across the rational surface [5]. The terms Γ_{BS}, Γ_{GGJ}, Γ_{pol} and Γ_{EC} represent effects of the bootstrap current, the field line curvature [6], the ion polarization current [7] and EC current drive and the EC current effect [8]. B_{p}, η, ε_{s}, β_{ps}, ρ_{pi} and ρ_{s} are the poloidal magnetic field, the neoclassical resistivity, the inverse aspect ratio, the local poloidal beta, the poloidal Larmor radius normalized by minor radius and the rational surface position, respectively. The scale lengths, L_{q} and L_{p}, are defined as $L_{\mathrm{q}} = q(\mathrm{d}q/\mathrm{d}\rho)^{-1}$ and $L_{\mathrm{p}} = -p(\mathrm{d}p/\mathrm{d}\rho)^{-1}$. Figure 1 shows the model of EC modulation in phase with island rotation. The localization efficiency of EC current, η_{EC}, is given as in [8]

$$\eta_{\mathrm{EC}} = \frac{\int \mathrm{d}\rho \oint_{2\pi}^{\mathrm{d}\alpha} \cos(m\alpha) \langle\langle j_{\mathrm{EC}} \rangle\rangle}{\int \mathrm{d}\rho \oint_{2\pi}^{\mathrm{d}\alpha} \langle\langle j_{\mathrm{EC}} \rangle\rangle}, \tag{7}$$

and is calculated numerically according to the EC current profile on the flux surface of an island structure, which is assumed to be reconstructed on the ρ coordinate. The value

author's e-mail: yamazaki@ees.nagoya-u.ac.jp

*) This article is based on the presentation at the 21st International Toki Conference (ITC21).

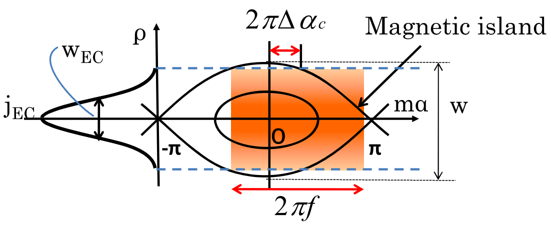

Fig. 1 Model of EC modulation injection in phase with island rotation. Normalized modulation width is f, and the normalized phase lag from the O-point of magnetic island is $\Delta\alpha_c$.

Table 1 Coefficients of each term in the modified Rutherford equation used here.

k_c	1.2
k_{BS}	4.5
k_{GGJ}	1
k_{pol}	1
k_{EC}	2.9

Table 2 Plasma parameter used here for ITER

R_0: major radius (m)	6.2
a: minor radius (m)	2
B_{t0}: troidal field at R_0 (T)	5.3
I_p: plasma current (MA)	15
κ: Elipticity	1.7
δ: Triangurality	0.3
$\langle n_e \rangle$ (10^{20}m^{-3})	1
$\langle T_e \rangle$ (keV)	10.4
$\langle T_i \rangle$ (keV)	9.5
β_N	2.1

of $\langle\langle j_{EC} \rangle\rangle$ is the flux surface averaged value of j_{EC} on the island structure. The value of I_{EC} in Eq. (6) is the total time-averaged amount of the EC current. The peaked EC current is I_{EC}/f. The EC current profile is modeled by the Gaussian distribution

$$j_{EC} = j_{EC0} \exp\left(-C\left(\frac{\rho - \rho_s}{W_{EC}}\right)^2\right), \tag{8}$$

where $C = 4\ln 2$, j_{EC0} is calculated from total EC current I_{EC}. The normalized peak radius of the EC current profile, ρ_{EC}, is assumed to be equal to ρ_s, and the EC injection width W_{EC} is the full-width at half maximum of the EC current profile.

3. Numerical Results

The coefficients of each term in the modified Rutherford equation used here are shown in Table 1. Table 2 shows parameters of the ITER plasma analyzed in this paper. Here, we used almost same parameters as those in the reference [2] based on the JT-60 experiments.

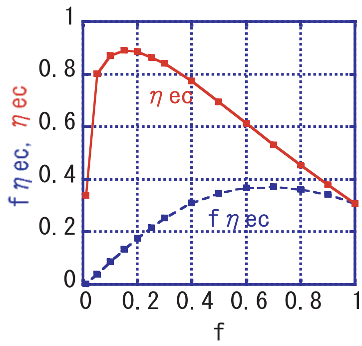

Fig. 2 EC current efficiency η_{ec} (solid lines) and $f\eta_{ec}$ (broken lines) as a function of EC modulation width f in the case of $\Delta\alpha_c = 0$ and $W_{EC}/W = 0.4$.

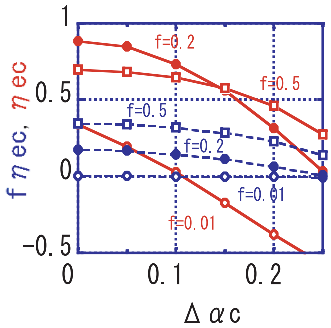

Fig. 3 EC current efficiency η_{ec} (solid lines) and $f\eta_{ec}$ (broken lines) as a function of EC injection phase lag $\Delta\alpha_c$ for f = 0.02, 0.2 and 0.3. The ratio of EC current width to the 2/1 island width is assumed to be 0.4.

3.1 NTM stabilization by modulated ECCD

Figure 2 shows the change of the ECCD control efficiency η_{ec} and $f\eta_{ec}$ as a function of EC modulation width f. The efficiency η_{ec} with the assumption of constant time-averaged EC current is highest when f is about 0.2. On the other hand, the efficiency $f\eta_{ec}$ for the case of constant peaked EC current density is maximized at around $f = 0.6$, which is consistent with the results of Ref. [9].

The changes in η_{ec} and $f\eta_{ec}$ as a function of the normalized EC injection phase lag $\Delta\alpha_c$ from the O-point of magnetic island are shown in Fig. 3. For smaller phase lag, η_{ec} and $f\eta_{ec}$ become larger. In the case of $f = 0.01$, η_{ec} is about 0.3 when $\Delta\alpha_c$ is nearly equal to zero. When $\Delta\alpha_c$ is larger than 0.10, η_{ec} becomes a negative value. For $f = 0.5$ (half of the magnetic island), η_{ec} and $f\eta_{ec}$ are about 0.7 and 0.4, respectively, and for $f = 0.20$, a large value $\eta_{ec} = 0.9$ (a moderate value $f\eta_{ec} = 0.2$) can be achieved. Therefore, when EC total time-averaged current, but not EC peaked current density, is fixed, NTM can be stabilized with smaller EC time-averaged current if EC modulation width is around 0.2 and the phase lag is smaller than 0.1.

Temporal evolutions of magnetic island width and center electron temperature in ITER plasma as functions of EC modulation width f and phase lag $\Delta\alpha_c$ are shown

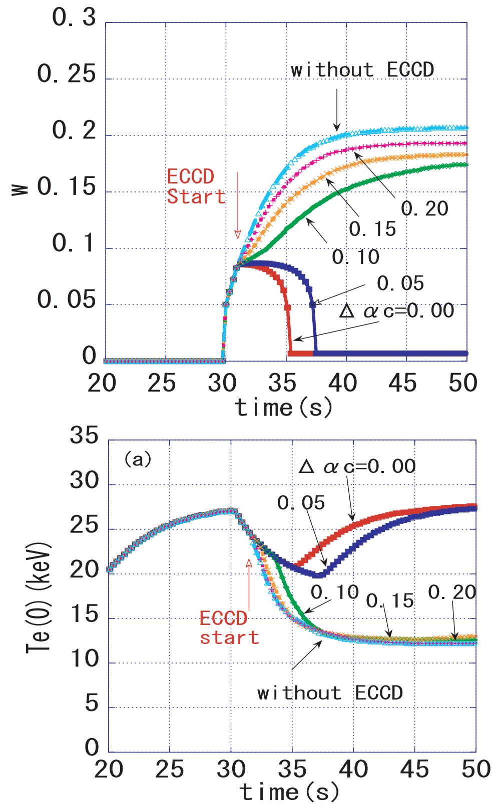

Fig. 4 Temporal evolution of (a) magnetic island width W and (b) center electron temperature $T_e(0)$ for EC modulation width f = 0.2 in the case of $\Delta\alpha_c$ = 0 and W_{EC}/W = 0.4.

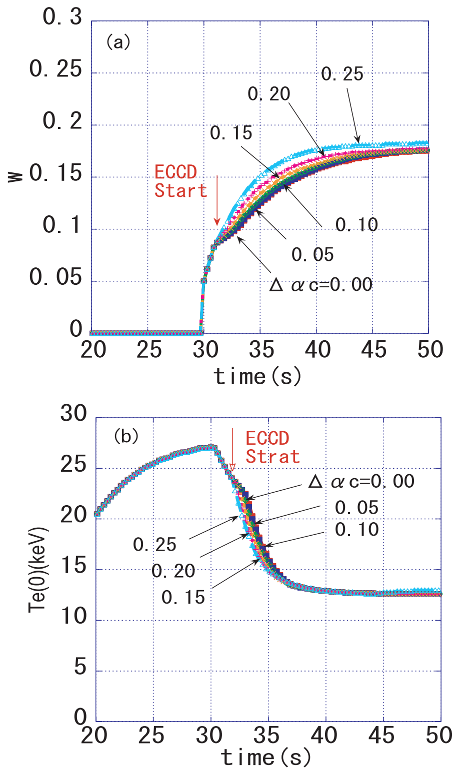

Fig. 5 Temporal evolution of (a) magnetic island width W and (b) center electron temperature $T_e(0)$ for EC modulation width f = 0.5. The ratio of EC current width to the 2/1 island width is assumed to be 0.4.

in Figs. 4 and 5. The total time-averaged EC current I_{EC} is fixed to 70 kA, and the peaked EC current density is five times (Fig. 4) or two times (Fig. 5) larger than that of the non-modulation case. According to Fig. 2, the EC control efficiency becomes highest when the lag in the EC injection phase from O-point of magnetic island is smaller and EC modulation width is around 20%. NTM can be stabilized and the electron temperature is recovered when $\Delta\alpha_c < 0.10$ and $f \sim 0.2$.

The fusion energy gain Q value is shown in Table 3. Here, the simplified relationship between total EC current and the EC power, I_{EC} [kA] = 415E_{EC} [MW], is used for 2/1 NTM island stabilization [9]. Here we assume that even in the case of ECCD modulation operation, the time-averaged EC current I_{EC} is assumed to be explained by this equation with time-averaged EC electric power E_{EC}. The possible peaked current density is proportional to I_{EC}/f, and the required capacity (kVA) of electric power facility might be $1/f$ times larger than the non-modulation one. However, the required time-averaged ECCD power in the modulation case is the same as that in the non-modulation case. In the reactor, not only ECCD power capacity but also the required time-averaged stabilization electric power is a key parameter.

Q becomes larger than 10 when NTM is stabilized completely. But for the other case, the expected Q is smaller than 2.0 in this simulation profile.

Table 3 Fusion energy gain Q of ITER plasma with NTM stabilization by ECCD (I_{EC} = 70 kA).

	f = 0.01	f = 0.20	f = 0.50
	I_{EC}/f = 7000 kA	I_{EC}/f = 350 kA	I_{EC}/f = 140 kA
$\Delta\alpha_c$ = 0.00	1.6	12.3	1.7
$\Delta\alpha_c$ = 0.05	1.6	12.3	1.7
$\Delta\alpha_c$ = 0.10	1.6	1.7	1.7
$\Delta\alpha_c$ = 0.15	1.0	1.6	1.7
$\Delta\alpha_c$ = 0.20	1.0	1.6	1.7
$\Delta\alpha_c$ = 0.25	1.0	1.6	1.7

4. Summary

In this simulation, 2/1 NTM analysis and its stabilization by ECCD in ITER have been carried out based on the modified Rutherford equation. NTM can be stabilized by modulated ECCD easily, when the normalized EC modulation width to the magnetic island width is around 20%, and the normalized EC injection phase lag from the O-point of the magnetic island is smaller than 10%. This is because the EC control efficiency is highest at the modulation width of 0.2 when the total time-averaged EC current is fixed. If the peaked EC current is fixed, the control efficiency might be highest at the modulation width of around 0.6. The simulation clarified that the fusion gain Q is reduced to less than 2 due to the destabilization of 2/1 NTM. In order to make high Q value ($Q > 10$) in ITER, NTM should be stabilized.

In this paper, the analysis was mainly based on the constant time-averaged EC current and power. When the peaked EC current is fixed, the stabilization efficiency might be maximized at around $f \sim 0.6$ instead of 0.2 as shown in Fig. 2, which will be checked in the future.

[1] Y. Takahashi, K. Yamazaki *et al.*, Journal of Physics: Conference Series **123**, 012036 (2008).
[2] N. Hayashi, A. Isayama *et al.*, J. Plasma Fusion Res. **80**, 605 (2004).
[3] K. Yamazaki, T. Amano *et al.*, Nucl. Fusion **25**, 1543 (1985).
[4] R.E. Waltz, G.M. Staebler *et al.*, Nucl Fusion **44**, 477 (2004).
[5] H.P. Furth, P.H. Rutherford *et al.*, Phys. Fluids **16**, 1054 (1973).
[6] M. Kotschenreuther, R.D. Hazeltine *et al.*, Phys. Fluids **28**, 899 (1985).
[7] H.R. Wilson *et al.*, Phys. Plasmas **3**, 248 (1996).
[8] C.C. Hegna and J.D. Callen, Phys. Plasmas **4**, 2940 (1997).
[9] N. Hayashi *et al.*, Nucl. Fusion **44**, 477 (2004).